Langmuir
Article
pubs.acs.org/Langmuir

Interaction between Langmuir and Langmuir−Blodgett Films of Two Calix[4]arenes with Aqueous Copper and Lithium Ions

Faridah L. Supian,[†] Tim H. Richardson,*[,†] Mary Deasy,[‡] Fintan Kelleher,[‡] James P. Ward,[‡] and Vickie McKee[§]

[†]*Department of Physics & Astronomy, University of Sheffield, Hounsfield Road, Sheffield S37RH, United Kingdom,* [‡]*Department of Science, Institute of Technology Tallaght (ITT Dublin), Dublin 24, Ireland, and* [§]*Department of Chemistry, Loughborough University, Loughborough, Leicestershire LE113TU, United Kingdom*

Received February 25, 2010. Revised Manuscript Received April 6, 2010

The binding interactions between aqueous copper (Cu^{2+}) and lithium (Li^{+}) ions and Langmuir monolayers and Langmuir−Blodgett (LB) multilayers have been investigated by studying surface pressure−area ($\Pi-A$) isotherms and surface potential−area ($\Delta V-A$) behavior in order to find the effective dipole moment, $\mu_{\perp}$, of the calixarene molecules in the uncomplexed and complexed states. The orientation of both calix[4]arenes, namely, 5,11,17,23-tetra-*tert*-butyl-25,27-diethoxycarbonyl methyleneoxy-26,28-dihydroxycalix[4]arene and 5,17-(9H-fluoren-2-yl)methyleneamino)-11,23-di-*tert*-butyl-25,27-diethoxycarbonyl methyleneoxy-26,28-dihydroxycalix[4]arene, is such that the plane of the calix ring is parallel with the plane of the water surface regardless of the ion content of the subphase. The Gibbs equation was used to interpret the adsorption of ions with both calix[4]arenes as a function of the concentration. Effective dipole moments have been calculated from surface potential values using the Helmholtz equation. In this work, new LB films have been prepared employing two novel amphiphilic calix[4]arene derivatives bearing different upper rim substituents. Thus, the effect of modifiying the upper rim has been observed. The results have shown that these calixarenes may be useful components of ion sensors.

1. Introduction

Calix[4]- and calix[8]arenes, appropriately substituted on their upper and lower rims, are known to form highly uniform Langmuir monolayer films on a water subphase and also well-ordered transferred Langmuir−Blodgett (LB) multilayers on various solid substrates. Interest in such films has developed in the areas of gas sensing, ion binding,[1] and pyroelectric heat detection.[2] Calixarenes are unusual among small organic molecules in that they exhibit relatively high thermal stability with melting points typically around 250−280 °C.[3] Furthermore, this is particularly exceptional among LB film forming materials which commonly consist of more traditional amphiphiles such as long-chain carboxylic acids or phospholipids possessing melting points closer to the range 60−80 °C.[4] For these combined reasons, calixarenes represent a family of materials attracting increasing interest in the nanoscience community.

Previous research in this area has included the interaction between Langmuir films of calix[*n*]arenes and various cations, anions, and amines.[1,5,6] Turshatov et al. studied the behavior of a calix[4]resorcinarene with copper ions, although this work did not include LB films or compare differently substituted (upper rim) molecules.[7] Weis et al. reported the interaction of dopamine with a calix[4]resorcinarene in the form of an LB monolayer using surface potential, ΔV, and found that the binding depends on the orientation of the calixarene in the monolayer.[8] Research carried out by Nabok et al. revealed the behavior of calix[4]resorcinolarene using surface pressure−area ($\Pi-A$) isotherms and surface potential−area ($\Delta V-A$) data in order to investigate the adsorption mechanism of four different upper rims of calix[4]resorcinolarene.[9]

Derivatization of calixarenes is possible at either the upper or lower rim as in Figure 1, and usually has the added effect of locking the calixarene into one conformation. Some of the earliest work in this area involved converting the phenolic oxygens of the parent calixarenes to their acetates.[10] McKervey et al. produced a group of calixaryl esters and ketones and investigated their binding properties. The group devised simple, yet highly effective, synthetic routes for this group of compounds, on which many subsequent derivatives were based.[11]

The derivatization of calixarenes has been reported to influence strongly on the complexation affinity for metal ion guests. Selectivity for alkali metal cations is known to be altered by changing the *p*-substituents.[12] In recent years, there has been an increase in the level of interest in the generation of ultrathin organic films, encapsulating ionophoric macromolecules, using techniques such as LB deposition. In 2009, Wang et al. reported

*To whom correspondence should be addressed. Telephone: +44114 22 23508. Fax: +44114 22 24280. E-mail: t.richardson@sheffield.ac.uk.

(1) Hassan, A. K.; Nabok, A. V.; Ray, A. K.; Davis, F.; Stirling, C. J. M. *Thin Solid Films* **1998**, *686*, 327.
(2) McCartney, C. M.; Richardson, T.; Greenwood, M. B.; Cowlam, N. *Supramol. Sci.* **1997**, *4*, 385.
(3) Boehmer, V.; Marschollek, F.; Zetta, L. *Org. Chem.* **1987**, *52*, 3200.
(4) Roberts, G. G. *Langmuir−Blodgett Films*; Plenum Press: New York, 1990.
(5) Pathak, R. K.; Ibrahim, S. M.; Chebrolu, P. *Tetrahedron Lett.* **2009**, *50*, 2730.
(6) Joseph, R.; Ramanujam, B.; Acharya, A.; Rao, C. P. *Tetrahedron Lett.* **2009**, *50*, 2735.
(7) Turshatov, A. A.; Melnikova, N. B.; Semchikov, Y. D.; Ryzhkina, I. S.; Pashirova, T. N.; Mobius, D.; Zaitsev, S. Y. *Colloids Surf., A* **2004**, *240*, 101.
(8) Weis, M.; Janicek, R.; Cirak, J.; Hianik, T. *J. Phys. Chem. B* **2007**, *111*, 10626.
(9) Nabok, A. V.; Lavrik, N. V.; Kazantseva, Z. I.; Nesterenko, B. A.; Markovskiy, L. N.; Kalchenko, V. I.; Shivaniuk, A. N. *Thin Solid Films* **1995**, *259*, 244.
(10) Bocchi, V.; Foina, D.; Pochini, A.; Ungaro, R.; Andreetti, G. D. *Tetrahedron Lett.* **1982**, *38*, 371.
(11) Neu, F. A.; Collins, E. M.; Deasy, M.; Ferguson, G.; Harris, S. J.; Kaitner, B.; Lough, A. J.; McKervey, M. A.; Marques, E.; Ruhl, B. L.; Schwing, M. J.; Seward, E. M. *J. Am. Chem. Soc.* **1989**, *111*, 8681.
(12) *Calixarenes 2001*; Asfari, Z., Bohmer, V., Harrowfield, J., Vicens, J., Eds.; Kluwer Academic: Dordrecht, 2001; p 683.

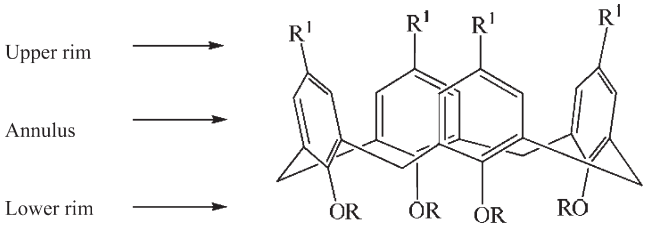

Figure 1. Calix[4]arene with three distinct regions.

that a *p-tert*-butylthiacalix[4]arene LB film modified electrode was found to greatly improve the measuring sensitivity of the Ag^+ ion over traditional glassy electrode systems.[13]

In this investigation, the two calix[4]arenes are different only in that one material contains a mixed upper rim system, consisting of two alkyl groups and two highly conjugated groups, whereas the other contains only alkyl groups in the upper rim positions. A preliminary comparison of the shift in the UV−visible absorption spectrum of these calixarene as a result of their complexation with various metal salts indicated that their interaction with Cu^{2+} and Li^+ would be of great interest in the context of identifying ion-sensing materials. Therefore, the two ions were chosen in this study to observe their interaction with these calixarenes at different ion concentrations in terms of ΔV and effective dipole moment, $\mu_\perp$, properties of Langmuir monolayer and deposited LB films to verify that these calixarenes are suitable candidates for ion sensing.

2. Materials and Methods

2.1. Materials, Synthesis, and Compound Data. In Figure 2, calixarenes **A** and **B** are shown, and their syntheses are discussed in the next section.

The synthesis of distal derived calixarenes with ionophoric ligating groups, such as compound **A**, is well-known. Hence, **A** was prepared in three steps as follows. *p-tert*-Butylcalix[8]arene (cyclic octamer) was first prepared by the modified Munch procedure[14,15] from *p-tert*-butylphenol and paraformaldehyde in the presence of KOH and was isolated as a white powder, in 70% yield. This was then subjected to molecular mitosis[16,17] to form *p-tert*-butylcalix[4]arene (cyclic tetramer). Sodium hydroxide was the base of choice due to the template effect between the cavity size of the tetramer and the size of the Na^+ cation, which induced formation of the tetramer in a 71% yield. The reaction of *p-tert*-butylcalix[4]arene with ethyl bromoacetate under conventional conditions for alkylation (K_2CO_3 as base in acetonitrile as solvent) resulted in the expected distal-dialkyl derivative **A** with terminal ester groups.[11] Pathak et al. have very recently reported the synthesis of a series of lower rim 1,3-diderivatived calix-[4]arene compounds possessing Schiff base cores with binding to Zn^{2+} ion taking place at the Schiff base binding sites.[5] A diderivatized calix[4]arene based fluorescent sensor has also recently been reported by Rao et al.[6] The sensor was found to be highly selective for the Cu^{2+} ion over a range of metal ions tested.

We recently published the synthesis of a new upper rim derived calixarene compound with Schiff base ligating groups which showed good affinity for Fe(III).[18,19] In this study, we have synthesized another novel calix Schiff base compound for incorporation into an LB film.

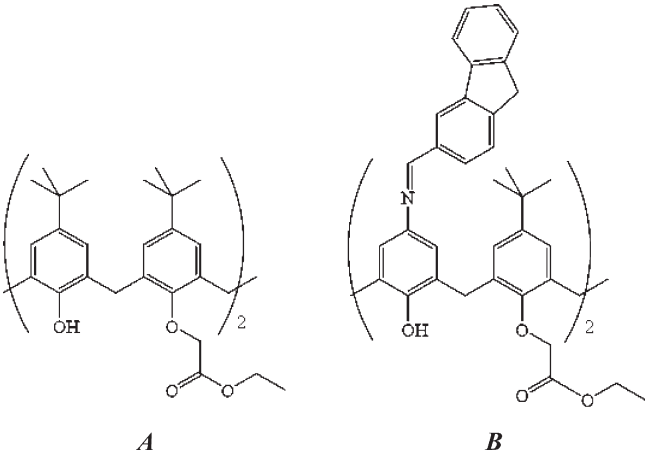

A *B*

Figure 2. Calixarenes **A** and **B**: 5,11,17,23-tetra-*tert*-butyl-25,27-diethoxycarbonyl methyleneoxy-26,28-dihydroxycalix[4]arene and 5,17-(9H-fluoren-2-yl)methyleneamino)-11,23-di-*tert*-butyl-25,27-diethoxycarbonyl methyleneoxy-26,28-dihydroxycalix[4]arene.

The upper rim derived Calix-Schiff **B** was synthesized by the synthetic route shown in Figure 3. Nitro-dealkyation was conducted in accordance with the literature procedure of Verboom et al.[28] Reduction of the nitro calix[4]arene to the calix[4]arene diamine was achieved by hydrogenation, at 2 atm of pressure, in ethanol in the presence of Raney-Nickel in almost quantitative yield (99%), as published by our group previously. The calixarene diamine was heated to reflux temperature in ethanol with a 5 molar excess of fluorenecarboxaldehyde. A pink red colored solid was recrystallized from chloroform/methanol in a 63% yield.

The ^{1}H NMR spectrum of **B** showed a sharp singlet at 8.43 ppm for the newly formed imine proton. The remaining protons on the fluorene component resonated between 8.10 and 7.30 ppm as multiplets, resulting from coupling between the protons on each aromatic ring, while the phenolic OH protons appeared as a singlet at 7.65 ppm. The calixarene aromatic protons were observed as a multiplet at 7.02−7.00 ppm. The bridging CH_2 of the fluorene resonated as a singlet at 3.94 ppm, while the *tert*-butyl protons appeared as a singlet at 1.12 ppm. The imine CH appeared at 158.2 ppm in the ^{13}C NMR spectrum of **B**, while the ester C=O resonated at 169.8 pm. A total of 10 signals, between 151.8 and 128.7 ppm, were observed for the calixarene and fluorene ArC_q atoms. The ArCH carbons of the fluorene moiety resonated between 144.1 and 126.5 ppm, while those of the calixarene moiety were observed at 125.6 and 125.2 ppm. The bridging CH_2 of the fluorene appeared at 37.2 ppm, while the calixarene bridging CH_2 resonated at 34.5 ppm. The *tert*-butyl CH_3 appeared at 31.7 ppm. An absorbance at 3442 cm^{-1} was observed in the IR spectrum of **B** for the phenolic OH, while the ester C=O absorbed at 1752 cm^{-1} and the imine C=N absorbed at 1626 cm^{-1}.

2.1.1. Preparation of 5,11,17,23-Tetra-tert-butyl-25,27-diethoxycarbonyl Methyleneoxy-26,28-dihydroxycalix[4]arene [A]. The calixarene diester derivative (**A**) was prepared in 81% yield following a procedure similar to that described by McKervey et al.[11] mp: 172−174 °C (lit.[19] 182−184 °C). R_f: 0.21 (70% DCM/petroleum ether). υ_{max}/cm^{-1} (KBr): 3427 (polymeric OH str.), 2962, 2902, 2864 (C−H str.), 1751 (C=O str). δ_H/ppm (300 MHz, $CDCl_3$): 7.07 (2H, s, phenolic OH), 7.02 (4H, s, ArCH), 6.82 (4H, s, ArCH), 4.72 (4H, s, $-O-\underline{CH_2}-CO_2CH_3$), 4.45 (4H, d, $Ar-\underline{CH_2}-Ar$, J = 12.0 Hz), 4.30 (4H, q, $\underline{CH_2}CH_3$, J = 7.0 Hz), 3.32 (4H, d, methylene, J = 12.0 Hz), 1.33 (6H, t, $CH_2\underline{CH_3}$, J = 7.0 Hz), 1.30 and 1.26 (2 × 18H, s, *tert*-butyl). δ_C/ppm (75 MHz, $CDCl_3$): 169.2 (ester C=O), 150.7 (ArC_q-OH), 150.3 (ArC_q-OR),

(13) Wang, F.; Liu, Q.; Wu, Y.; Ye, B. *Electroanal. Chem.* **2009**, *630*, 49.
(14) Gutsche, C. D.; Dhawan, B.; No, K. H.; Muthukrishman, R. *J. Am. Chem. Soc.* **1981**, *103*, 3782.
(15) Munch, J. H.; Gutsche, C. D. *Org. Synth.* **1990**, *68*, 233.
(16) Gutsche, C. D.; Levine, J. A.; Sujeeth, P. K. *J. Org. Chem.* **1985**, *50*, 5802.
(17) Schmitt, P.; Beer, P. D.; Drew, M. G. B.; Sheen, P. D. *Angew. Chem., Int. Ed. Engl.* **1997**, *36*, 1840.
(18) Supian, F. L.; Richardson, T. H.; Deasy, M.; Kelleher, F.; Ward, J. P.; McKee, V. *Sains Malays.* **2009**, *39*, 423.
(19) Ward, J. P. Ph.D. Thesis, Institute of Technology Tallaght, 2009.

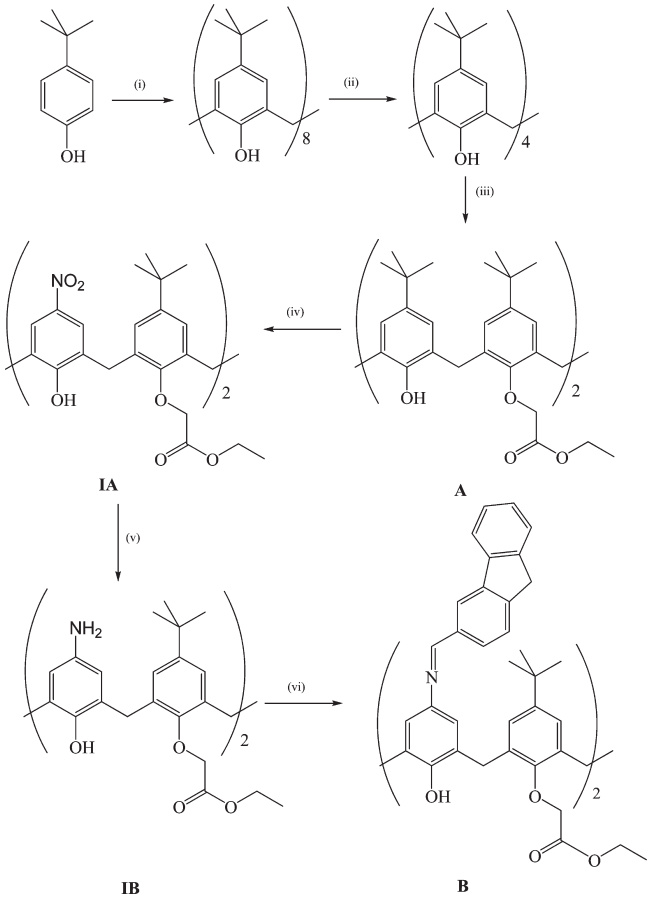

Figure 3. Reaction conditions: (i) HCHO, KOH, xylene; (ii) NaOH, Ph_2O; (iii) $BrCH_2COOEt$, K_2CO_3,, CH_3CN; (iv) HNO_3, CH_3COOH, CH_2Cl_2; (v) H_2 (2 atm), Ra/Ni, EtOH; (vi) fluorene-carboxaldehyde, EtOH.

147.1, 141.5 (ArC_q-*tert*-butyl), 132.5, 128.0 (ArC_q), 125.7, 125.1 (ArCH), 72.4 (Ar−O-$\underline{C}H_2$), 61.2 (ester −$\underline{C}H_2CH_3$), 33.9, 33.7 (C_q *tert*-butyl), 31.8 (Ar−$\underline{C}H_2$−Ar), 31.6, 31.0 (*tert*-butyl CH_3), 14.2 (ester −$CH_2\underline{C}H_3$).

2.1.2. Preparation of 5,17-Dinitro-11,23-ditert-butyl-25,27-diethoxycarbonyl Methyleneoxy-26,28-dihydroxycalix[4]arene [*IA*]. Nitro dealkylation of the diethyl ester calixarene I was achieved following the literature procedure of McGinley et al.[29] using nitric acid in a mixture of acetic acid and dichloromethane. Recrystallization from methanol afforded a yellow solid (4.32 g, 21%). mp: 197−199 °C (lit.[20] 198−200 °C). R_f: 0.42 (70% DCM/pet. ether);. υ_{max}/cm^{-1} (KBr): 3289 (phenolic OH), 2967; 2868 (aliphatic CH), 1727 (C═O), 1510; 1336 (NO_2). δ_H/ppm (300 MHz, $CDCl_3$): 8.94 (s, 2H, phenolic OH), 7.96 (s, 4H, ArCH), 7.03 (s, 4H, ArCH), 4.72 (s, 4H, $-OCH_2CO$), 4.51 (d, 4H, Ar−CH_2−Ar), 4.32 (q, 4H, ester CH_2), 3.44 (d, 4H, Ar−CH_2−Ar), 1.36 (t, 6H, ester CH_3), 1.09 (s, 18H, *tert*-butyl). δ_C/ppm (75 MHz, $CDCl_3$): 168.6 (C═O), 158.8 (C_qAr−OH), 151.8 (ArC_q−OR), 144.8 (C_qAr-*tert*-butyl), 141.8 (C_qAr-NO_2), 131.1 (ArC_q), 128.9 (ArC_q), 126.8, 125.4 (ArCH), 73.5 ($-OCH_2CO$), 60.8 (ester CH_2), 33.9 (C_q-*tert*-butyl), 31.7 (Ar−$\underline{C}H_2$−$\underline{A}r$), 29.9 (*tert*-butyl CH_3), 14.0 (ester CH_3).

2.1.3. Preparation of 5,17-Diamino-11,23-ditert-butyl-25,27-diethoxycarbonyl Methyleneoxy-26,28-dihydroxycalix[4]arene [*IB*]. To a suspension of dinitro calixarene I**A** (2 g, 2.4 mmol) in ethanol (200 mL) was added a catalytic amount of Raney-Nickel. The mixture was placed on a hydrogenator for 2 h (2 atm) then filtered through a bed of Celite. The solvent was removed in vacuo to leave compound I**B** as a pink solid (1.97 g, 99%). mp: 175−177 °C. R_f = 0.75 (DCM/pet. ether). υ_{max}/cm^{-1} (KBr): 3310 (phenolic OH and NH), 1746 (C═O). δ_H/ppm (300 MHz, $CDCl_3$): 7.12 (s, 2H, phenolic OH), 7.01 (s, 4H, ArCH), 6.95 (s, 4H, ArCH), 6.30 (s, 4H, NH_2), 4.82 (s, 4H, $-OCH_2CO$), 4.52 (d, 4H, Ar−CH_2−Ar), 4.29 (q, 4H, −$C\underline{H}_2CH_3$), 3.21 (d, 4H, Ar−CH_2−Ar), 1.32 (t, 6H, −$CH_2C\underline{H}_3$), 1.24 (s, 18H, *tert*-butyl). δ_C/ppm (75 MHz, $CDCl_3$): 169.9 (C═O), 151.7 (C_qAr−OH), 147.2-(ArC_q−OR), 149.3 (C_qAr-*tert*-butyl), 141.8 (C_qAr−NO_2), 133.5 (ArC_q), 130.7 (ArC_q), 126.0, 116.2 (ArCH), 72.0 ($-O\underline{C}H_2CO$), 61.2 (ester CH_2), 34.2 (*tert*-butyl CH_3), 32.3 (Ar−$\underline{C}H_2$−$\underline{A}r$), 29.7 (*tert*-butyl CH_3), 14.2 (ester CH_3).

2.1.4. Preparation of 5,17-(9H-Fluoren-2-yl)methyleneamino)-11,23-ditert-butyl-25,27-diethoxycarbonyl Methyleneoxy-26,28-dihydroxycalix[4]arene [***B***]. To a solution of diamine I**B** (0.7 g, 0.95 mmol) in ethanol (60 mL) was added fluorene carboxaldehyde (0.97 g, 5 mmol), and the solution was heated at reflux temperature for 16 h and cooled. The solid residue was recovered by vacuum filtration and recrystallized from chloroform/methanol to give a red solid (0.66 g, 63%). mp: 271−273 °C. R_f: 0.41 (30% EtOAc/pet. ether); $C_{72}H_{70}N_2O_8 \cdot H_2O$ requires C, 77.95%, H, 6.54%, N, 2.53%; found C, 77.62% H, 6.46% N, 2.52%. ES^+ for $C_{72}H_{70}N_2O_8$, expected [M+H]: 1010.5; observed [M+1]: 1010.5. υ_{max}/cm^{-1} (KBr): 3442 (phenolic OH), 2960; 2927 (aliphatic CH), 1626 (C═N), 1752 (C═O). δ_H/ppm (300 MHz, $CDCl_3$): 8.43 (s, 2H, a), 8.10 (s, 2H, b), 7.84−7.76 (m, 6H, c, d, e), 7.65 (s, 2H, phenolic OH), 7.57−7.54 (m, 2H, f), 7.41−7.30 (m, 4H, g, h), 7.02−7.00 (m, 8H, ArCH (calix)), 4.83 (s, ArC_q−O−$C\underline{H}2$−O−), 4.58−4.54 (d, 4H, Ar−CH_2−Ar (calix)), 4.37−4.30 (q, 4H, ester CH_2), 3.94 (s, 4H, Ar−CH_2−Ar (fluorene)), 3.45−3.41 (d, 4H, Ar−CH_2−Ar (calix)), 1.38−1.34 (t, 6H, ester CH_3), 1.12 (s, 18H, *tert*-butyl). δ_C/ppm (75 MHz, $CDCl_3$): 169.8 (C═O), 158.2 (imine CH), 151.8 (ArC_q−OH), 148.2 (ArC_q-OR), 144.5 (C_qAr-*tert*-butyl), 144.1, 141.4, 139.8, 138.2, 126.5 (C_qAr (fluorene)), 132.9, 128.7 (C_qAr (calix)), 129.7, 127.7, 127.3, 124.7, 121.5, 120.8, 120.3 (ArCH (fluorene)), 125.6, 125.2 (ArCH(calix)), 72.6 (ArC_q−O−$\underline{C}H_2$−O−), 61.7 (ester CH_2), 37.2 (Ar−CH_2−Ar (fluorene)), 34.5 (Ar−CH_2−Ar (calix)), 34.0 (C_q-*tert*-butyl), 31.7 (*tert*-butyl CH_3), 14.6 (ester CH_3).

2.2. X-ray Diffraction Study. Crystals of Calix-Schiff **B**·$^1/_2CHCl_3$, suitable for an X-ray diffraction study, were obtained from chloroform/methanol. Diffraction data were collected at 150(2) K on a Bruker Apex II CCD diffractometer. The structure was solved by direct methods and refined on F^2 using all the reflections.[20] All the non-hydrogen atoms were refined using anisotropic atomic displacement parameters, and hydrogen atoms were inserted at calculated positions using a riding model. There is disorder of the one of the upper rim substituents, modeled as 50% occupancy of two sites related by 180° rotation. There is also a 70:30 disorder of one of the terminal ethyl groups on the lower rim. The chloroform solvate molecule was refined with 50% occupancy.

$C_{72.50}H_{70.50}Cl_{1.50}N_2O_8$, triclinic, $P\bar{1}$, a = 13.6175(10), b = 13.7993(10), c = 19.4909(14) Å, α = 95.490(1), β = 90.115(1), γ = 119.018(1)°, V = 3183.2(4) Å^3, T = 150(2) K, λ = 0.71073 Å, Z = 2, 27 813 reflections measured, 12 471 unique (R_{int} = 0.0416), $wR2$ = 0.2669 (all data), $R1$ = 0.0749 ($I > 2\sigma(I)$). Crystallographic data have been deposited with the Cambridge Crystallographic Data Centre as supplementary publication no. CCDC 766050. (Copies of the data can be obtained, free of charge, on application to CCDC, 12 Union Road, Cambridge CB2 1EZ, U.K. (fax, +44-(0)1223-336033 or e-mail, deposit@ccdc.cam.ac.uk.)

2.3. Langmuir−Blodgett (LB) Studies. Solutions of **A** and **B** were prepared using chloroform as the solvent, and both concentrations were 0.2 mg/mL. Chromatography paper was used as the Wilhelmy plate in the trough for the measurement of ΔV. The deposition process followed the Y-type LB method.

A NIMA Langmuir trough (model 611) was used with a water subphase, namely, pure water (Elga Purelab water system, > 15 MΩ cm),

(20) Sheldrick, G. M. *Acta Crystallogr.* **2008**, *A64*, 112.

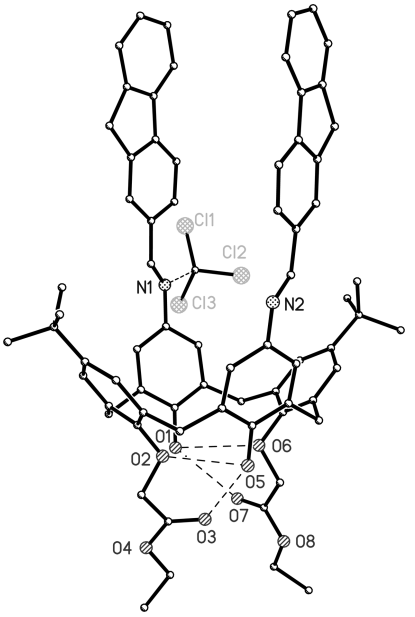

Figure 4. X-ray structure of Calix-Schiff $\mathbf{B}\cdot{}^{1}/_{2}CHCl_3$. Hydrogen bonds shown as dashed lines. Hydrogen atoms and the minor components of disorder have been omitted for clarity.

modified by the addition of copper (Cu^{2+}) and lithium (Li^{+}) salts. The Langmuir film material (**A** or **B**) was dispensed dropwise, using a Hamilton microsyringe, onto the surface of the subphase using volumes of 50 and 70 μL for **A** and **B**, respectively. A period of ~5 min was allowed for the solvent to evaporate. The barrier was then closed in order to record $\Pi-A$ isotherms and $\Delta V-A$ characteristics; the average compression speed was 100 $cm^2\ min^{-1}$ (the maximum area of the trough was 580 cm^2). Seven sets of data for different ion concentrations ranging from 0.0125 mM to 0.0750 mM were collected in order to observe the influence of the presence of Cu^{2+} and Li^{+} ions on the Langmuir film behavior.

In order to prepare the solution of Cu^{2+} ions with the required concentration, specific quantities of copper(II) perchlorate ($Cu(ClO_4)_2$) and pure water were mixed thoroughly in a beaker. Then the solution was poured into the trough. The same method was repeated using lithium perchlorate ($LiClO_4$) to obtain the Li^{+} ion solution.

For the purpose of measuring ΔV on transferred LB films, aluminum-coated glass substrates (Al thickness 210 nm) were used as substrates. Samples of 1 and 5 layers of LB films were deposited on the Al substrates using Y-type deposition with a chosen subphase concentration of 0.0375 mM.

2.4. Surface Potential, ΔV, Measurements. ΔV values were measured using a NIMA S-POT surface potential sensor (with an accuracy of ±2 mV) attached to the trough. The vibrating plate was aligned very near to the surface of the subphase while a counter electrode plate was placed in the bottom of the trough within the subphase. All experiments were performed at room temperature (21 ± 0.2 °C).

3. Results and Discussion

3.1. X-ray Diffraction Study. A perspective view of Calix-Schiff $\mathbf{B}\cdot{}^{1}/_{2}CHCl_3$ is shown in Figure 4. The partial-occupancy chloroform solvate is hydrogen-bonded to one of the imine nitrogen atoms (Table 1) but is outside the calixarene cavity (the H-bond is tangential to the calixarene ring). At the lower rim, the unsubstituted phenols each make bifurcated hydrogen bonds with neighboring phenylether and carbonyl oxygen atoms (table 1). The geometry of the calixarene ring is conventional, with the phenol groups tilted with respect to the mean plane of the four

Table 1. Hydrogen Bonds for $\mathbf{B}\cdot{}^{1}/_{2}CHCl_3$

D−H···A	*d*(D−H)	*d*(H···A)	*d*(D···A)	<(DHA)
O1−H1···O7	0.84	2.09	2.853(3)	151.3
O1−H1···O6	0.84	2.45	3.024(3)	126.5
O5−H5···O2	0.84	2.10	2.908(3)	160.4
O5−H5···O3	0.84	2.41	2.987(3)	126.8
C1S−H1S···N1	1.00	2.18	3.160(7)	165.9

methylene carbons by 78.49(7), 49.35(6), 71.07(7), and 47.51(8)° for the groups containing O1, O2, O5, and O6, respectively.

The two fluorene groups on the upper rim are orientated with their planes approximately parallel. They are intercalated with the fluorine groups of a second molecule to form centrosymmetric π-stacked dimers as in Figure 5. The mean interplanar distances for the stacked fluorenes are 3.41 Å for the outer pair and 3.47 Å for the inner pair; there are further $\pi-\pi$ interactions with neighboring dimers in the lattice.

3.2. Langmuir−Blodgett (LB) Studies: $\Pi-A$ Isotherms. As an example of the isotherm behavior, Figure 6 shows the $\Pi-A$ isotherms of **B** using three different Li^{+} concentrations. Upon compression, this calixarene undergoes two principal phase transitions: the first is a gas−liquid transition that begins at ~3.2 nm^2/molecule (for the pure water subphase), and the second, beginning at ~2.0 nm^2/molecule, can be thought of as a liquid−liquid or liquid−quasi solid rather than a liquid−solid transition since the compressibility of the high pressure phase is lower than is normally expected for a two-dimensional solid phase.

The well-defined isotherm is due to the highly amphiphilic nature of these calixarenes which are known to yield well-ordered Langmuir films at the air/water interface. The $\Pi-A$ isotherms are similar in terms of the phase structure, but increasing values of area per molecule, obtained via extrapolation of the solid phase region of the $\Pi-A$ isotherm to zero surface pressure, can be seen as the Li^{+} concentration increases. The value on pure water is ~2.0 nm^2, rising to ~2.2 and ~2.3 nm^2 as the concentration increases to 0.0125 and 0.0250 mM, respectively. Similarly, the take-off areas also increase in proportion to the Li^{+} concentration in the region ~3.2−3.6 nm^2. Furthermore, the isotherms cross over at ~16 mN/m; that is, the compressibility in the high pressure phase decreases with the Li^{+} ion concentration. These results show that the inclusion of the bound Li^{+} ion leads to a larger area per molecule and to a lower compressibility within the high pressure phase, indicating that the Langmuir layer properties are highly sensitive to the complexation interaction.

The area per molecule value for a pure water subphase is consistent with the formation of a calixarene monolayer as predicted using space-filling models (CPK molecular modeling) of **B** in which the orientation of the plane of the calixarene ring itself on the water surface is parallel to the plane of the water surface. The CPK molecular modeling, which is useful in predicting conformation and orientation, is a powerful method for comparison with the experimental results, and therefore, it was used widely here.[21] The two ethoxycarbonylmethyleneoxy and the two hydroxyl groups in the lower rim of both calixarenes are highly polar and therefore are expected to anchor the molecule to the water surface in this orientation, that is, with the plane of calixarene ring parallel to the plane of the water surface. The increase of the average area per molecule observed on the Li^{+} subphase indicates that the Li^{+} ion interacts with the monolayer. These observations are seen in both cases for **A** and **B**.

(21) Nostro, P. L.; Casnati, A.; Bossoletti, L.; Dei, L.; Baglioni, P. *Colloids Surf., A* **1996**, *116*, 203.

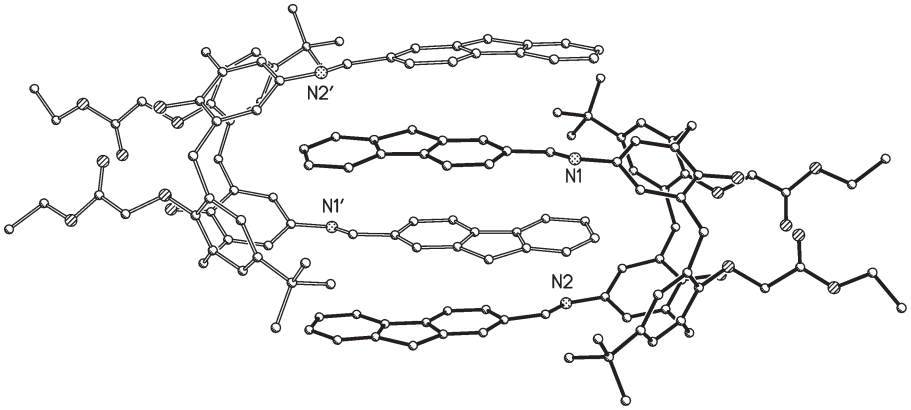

Figure 5. Intercalation of two molecules of Calix-Schiff **B**; the molecule on the left was generated by symmetry operation $-x$, $1-y$, $-z$.

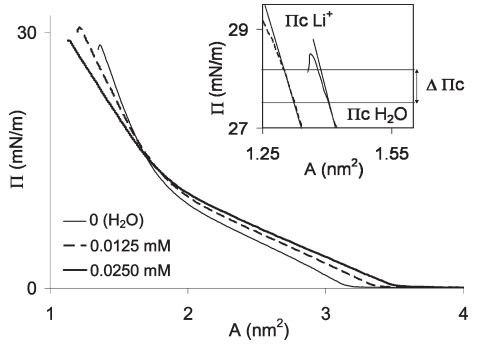

Figure 6. Pressure−area ($\Pi-A$) isotherm of **B** with three different concentrations of Li^+ ions in the subphase. Inset diagram showing the $\Delta\Pi_c = \Pi_c^{H_2O}-\Pi_c^{ions}$ where it shows the difference of the collapse pressure of water and Li^+ ion.

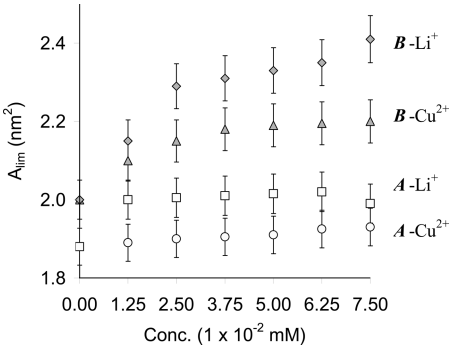

Figure 7. Dependence of A_{lim} for **A** and **B** on concentrations of Cu^{2+} and Li^+ ions.

Figure 7 shows that the limiting area per molecule, A_{lim}, increases as the concentration of ions in the subphase increases. Specifically, A_{lim} increases most rapidly for **B**−Li^+ and lowest by **A**−Cu^{2+}. For **A**−Cu^{2+}, it appears that very little increase in A_{lim} occurs, while for **A**−Li^+, the increase only occurs over a concentration range from 0 to 0.0125 mM. Generally, calixarene **B** shows a much stronger interaction compared to **A**.

It can be seen that A_{lim} for the monolayer increases as the salt concentration within the subphase increases. All the orientations of the calixarene rings of **A** and **B** are parallel (∥) to the water/air interface, as revealed by comparing the theoretical cross-sectional area values found using CPK modeling with the values of A_{lim} following the method described elsewhere.[22] Also, the −OH groups at the lower position of the calixarenes can form H-bonds with the water subphase, hence stabilizing the orientation at the air/water interface.[23]

3.3. Discriminating Cu^{2+} and Li^+ Ions within A and B. Liquid-vapor adsorption can be determined using interfacial tensions as a function of adsorbate concentration. In this case, the adsorbate is the Cu^{2+} or Li^+ ion which is adsorbed by the calixarene monolayer. Adsorption of Cu^{2+} and Li^+ can be calculated using the Gibbs equation:

$$\partial\gamma = -\Gamma^{ions} RTd \ln a_{ions} \quad (1)$$

where ions here refer to Cu^{2+} or Li^+, activity $a_{ions} \cong C_{ions}$ (dilute concentration in solution), and Γ^{ions} is near Γ^{ions}_{max}, forming the Gibbs−Shishkovsky equation.[7] Then, by plotting the change in collapse pressure ($\Pi_c^{H_2O} - \Pi_c^{ions}$) against $\ln(C_{ions})$, the gradient, m of the graph is given by

$$m \cong \Gamma^{ions}_{max} RT \quad (2)$$

where Γ^{ions}_{max} is the maximum adsorption of the ions, R is the universal gas constant, and T is temperature.

Figure 8 shows the corresponding graph of ($\Pi_c^{H_2O} - \Pi_c^{ions}$) versus $\ln(C_{ions})$. The y- axis values are found by deducting the Π_c of the calixarene monolayer on the subphase of aqueous ions from Π_c of the calixarene on the pure water subphase (Figure 6 inset). Each pair (calixarene−ion) yields a straight line graph whose gradients can be used to estimate the number of ions interacting with calixarene per unit area using eq 2. The gradients of those lines indicate the extent of the interaction behavior of each calixarene and each ion.

The Π_c value in the monolayer of calixarene **A** is only subtly affected by the presence of either Cu^{2+} or Li^+ ions. The gradients have opposite sign, since the Li^+ ions cause a reduction in the Π_c value and the Cu^{2+} cause an increase in its value. The resulting gradients are correspondingly very small, and from calculation using eq 2 they have values of -1.045×10^{-4} and 2.373×10^{-5} mol m^{-2} for Cu^{2+} and Li^+, respectively.

Calixarene **B** interacts much more strongly with both Cu^{2+} and Li^+ than calixarene **A**. The gradients have opposite sign, since the Cu^{2+} ions cause a reduction in the Π_c value measured from the isotherm, whereas the Li^+ ions cause an increase in the Π_c value. The interpretation of this is not straightforward but may be a reflection of the particular location where the binding of the cation takes place. It could be hypothesized that binding within

(22) Lonetti, B.; Nostro, P. L.; Ninham, B. W.; Baglioni, P. *Langmuir* **2005**, *21*, 2242.
(23) Maheswari, R.; Parthasarathi, R.; Dhathathreyan, A. *Colloid Interface Sci.* **2004**, *271*, 419.

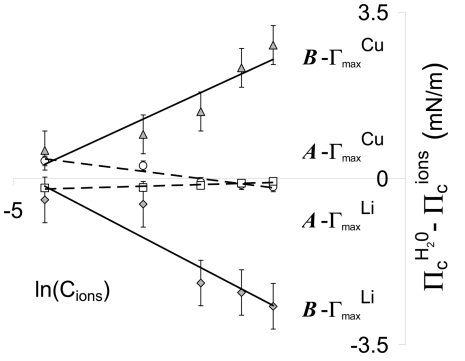

Figure 8. Plot of Γ_{max}^{ions} monolayer of **A** and **B** with different ions.

the calix[4]arene cavity or outside the cavity may lead to opposing effects on the collapse pressure. The gradient values signify the degree of interaction between the monolayer and the ions and are 3.802×10^{-4} mol m^{-2} for Cu^{2+} and -4.316×10^{-4} mol m^{-2} for Li^{+}.

3.4. Surface Potential, ΔV, and Effective Dipole Moment, $\mu_\perp$, Measurements on Langmuir Monolayer. ΔV is defined as the potential difference within the clean water surface and the coated surface in the subphase.[24] The Helmholtz equation states the relation between ΔV and $\mu_\perp$ for a Langmuir monolayer:

$$\mu_\perp = \varepsilon_0 \varepsilon A \Delta V \qquad (3)$$

where $\mu_\perp$ is the average dipole moment normal to the monolayer plane, ε_0 is the vacuum permittivity (8.854×10^{-12} C^2 N^{-1} m^{-2}), ε is the relative permittivity of the material between the electrodes, A is the area occupied by the molecule, and ΔV is the measured surface potential. Most researchers assume a value of $\varepsilon = 1$ for ultrathin films, since the thickness of the air gap between the monolayer and the vibrating electrode is very large compared to the thickness of the monolayer itself.

As an example, a graph of $\Pi-A$, $\Delta V-A$, and $\mu_\perp$ (inset diagram) for **B**$-Cu^{2+}$ at the concentration of 1.25×10^{-2} mM is displayed in Figure 9. Here, the ΔV values were obtained from experiment, while $\mu_\perp$ values were derived from eq 3. Referring to the $\Pi-A$ graph (Figure 6), in the gaseous state at large area per molecule (in the range 3.3−3.8 nm^2), ΔV does not increase above zero since the domains within the uncompressed Langmuir film are very sparsely distributed. Upon further compression, at ∼3.1 nm^2, ΔV and $\mu_\perp$ values begin to rise rapidly until they reach maximum due to the change in the orientation of the molecules. At this point (∼1.8 nm^2 for ΔV and ∼2.3 nm^2 for $\mu_\perp$), the optimum alignment of polar units within the calixarene layer has been achieved.

Referring to Figure 9, the $\Pi-A$ isotherm can be observed ∼2.3 nm^2, where the effective dipole moment $\mu_{\perp max}$ has reached its maximum value, ∼1.9 D corresponding to the onset of the gas−liquid phase transition. This can be explained by the fact, that during compression within the gaseous phase, the calixarene molecules undergo their greatest reordering/alignment. Upon reaching the gas−liquid transition, the molecules are virtually aligned as well as possible and little further improvement in ordering, which would lead to an increase in dipole moment, can be achieved throughout the remainder of the compression isotherm. Such behavior has been highlighted by previous authors for other calix[4]arenes.[8] Interestingly, a phase transition is observed at an area per molecule of ∼2.8 nm^2 in ΔV and $\mu_\perp$ inset plot which is not identifiable (or very slightly change) in the

(24) Taylor, D. M.; Oliveira, O. N.; Morgan, H. Surface potential of monomolecular films. IEEE Xplore, 1990.

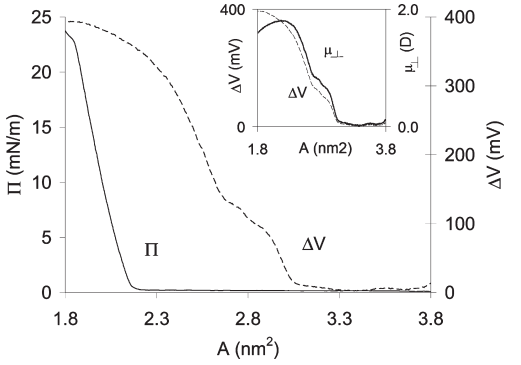

Figure 9. Relation between $\Pi-A$ (solid line) and $\Delta V-A$ (dotted line), while inset diagram shows $\Delta V-A$ (dotted line) and $\mu_\perp-A$ (solid line) of **B**$-Cu^{2+}$ at 1.25×10^{-2} mM.

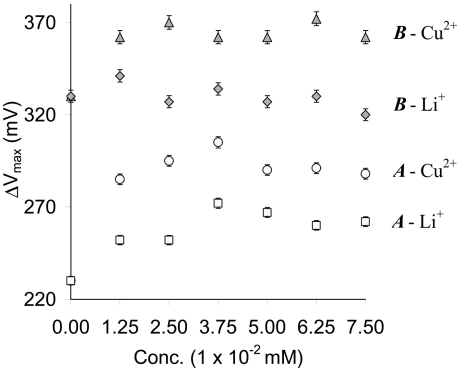

Figure 10. Dependence of ΔV_{max} of **A** and **B** interacting with Cu^{2+} and Li^{+} ions, respectively. Each point represents a maximum value for the corresponding concentration.

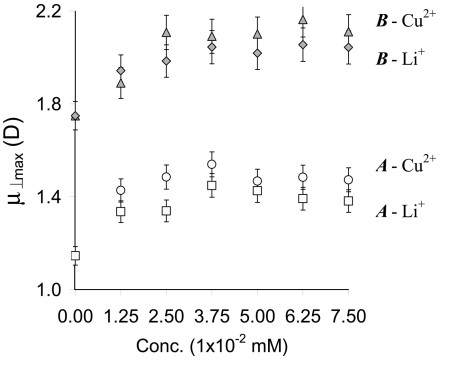

Figure 11. Dependence of $\mu_{\perp max}$ (D) for **A** and **B**.

$\Delta V-$A isotherm. The data sets of maximum values of ΔV and $\mu_\perp$ for both calixarenes were obtained over the concentration range $0-7.50 \times 10^{-2}$ mM and are shown in Figures 10 and 11.

Figure 10 shows the overall behavior of calixarenes **A** and **B** for the full range of subphase ion concentrations used for both Li^{+} and Cu^{2+} ions. The most abrupt increase for the ΔV_{max} can be observed for **A**$-Cu^{2+}$ and least with **B**$-Li^{+}$. When the salt is introduced into the subphase, the ions begin to interact with **A** and **B** until stabilization (equilibrium) is achieved, indicating the greatest number of ions that can bind with **A** and **B** has been reached. Thus, ion sensing of Cu^{2+} and Li^{+} ions using these calixarenes can be achieved over the ranges 0−0.0250 mM for **B**$-Cu^{2+}$ and 0−0.0375 mM for **A**$-Cu^{2+}$ and **A**$-Li^{+}$. The ΔV_{max} values measured for **B** are significantly higher than the corresponding values for **A**. This is due to the much larger molecular

Table 2. ΔV_{max} of A and B for the Monolayer Langmuir Film and Transferred LB Films[a]

	A			B		
subphase	air/water interface (mV)	LB film (mV), 1 layer	LB film (mV), 5 layers	air/water interface (mV)	LB film (mV), 1 layer	LB film (mV), 5 layers
water	230	152	87	330	226	120
Cu^{2+}	305	167	99	362	266	150
Li^{+}	272	157	91	334	255	122

[a] The errors in these measurements were approximately 2%.

dipole associated with the fluorenylmethylamino conjugated system compared to the simple alkylhydroxybenzene dipoles.

Figure 11 shows the corresponding derived $\mu_{\perp max}$ data. It must be emphasized that $\mu_{\perp}$ (from eq 3) depends on molecular area values, ΔV_{max} (Figure 10) and ε_0. The molecular dipole is made up of contributions from chemical groups within the substituted calixarene and the ring and also the interaction between the polar head groups, water, and aqueous ions. The molecular dipole moment for **B** is significantly larger than that of **A**; this is due to the presence of the extended region of conjugation within **B** in the form of the fluorenemethylamino system. Effective dipole moments measured by Weis et al.[8] and Nabok et al.[9] for similar calix[4]arene molecules that did not possess highly conjugated and polarizable electron systems were measured to be much lower than those in materials **A** and **B** here.

3.5. ΔV_{max} Measurements of Monolayer on Air/Water Interface and on Mono- and Multilayer on LB Film. In order to understand more the behavior and orientation of **A** and **B** on the various subphases, ΔV_{max} values for the floating Langmuir layers, transferred LB films comprising a monolayer and 5 layers deposited on a Al substrate, are compared in Table 2.

From Table 2, the values for the floating monolayer are higher than those for the LB films deposited on the Al substrate in all cases (water, Cu^{2+}, and Li^{+}). This is most probably due to the difference in average orientation of the calixarenes. At the air/water interface, the plane of the calixarene ring is parallel to the plane of the water surface owing to the strong interaction between the ethoxycarbonylmethyleneoxy groups and water and the hydroxyl groups and water, within the lower rim of the calixarene molecules.[25] The presence of the water subphase provides a very strong, dominant anchoring medium which has the effect of inducing a well-defined molecular orientation of the calixarene molecules within the monolayer.

However, the effect of the water subphase is absent from the deposited LB films and some disordering of the molecular dipoles is more likely to occur. Thus, the resulting electrical polarization and hence ΔV_{max} would be expected to be lower in the case of deposited films. Indeed, this increasing disorder is observed for multilayer (5 layers) LB films which exhibit smaller ΔV_{max} compared to monolayer LB films.

The degree of disorder thus grows as the polar molecular system progresses from the floating Langmuir film (little disorder) to the transferred LB monolayer (some disorder) to the deposited multilayer LB films (significant disorder).[23] If a perfect Y-type architecture resulted from the 5 layer LB films, then the measured ΔV_{max} from 4 sequentially deposited (Y-type) layers would cancel out.[26,27] Given that the observed ΔV_{max} LB monolayer values are always higher than those for the 5 layer LB film samples, it can be concluded that the entire multilayer film must be less aligned, *on average*, than the alignment within the monolayer.

4. Conclusions

The binding interactions between Cu^{2+} and Li^{+} ions (aqueous) and two calix[4]arenes, namely, 5,11,17,23-tetra-*tert*-butyl-25,27-diethoxycarbonyl methyleneoxy-26,28-dihydroxycalix[4]arene (material **A**) and 5,17-(9H-fluoren-2-yl)methyleneamino)-11,23-di-*tert*-butyl-25,27-diethoxycarbonyl methyleneoxy-26,28-dihydroxy-calix[4]arene (material **B**), have been investigated. The surface pressure−area isotherms reveal that the limiting areas per molecule lie in the range 1.9−2.5 nm^2 (depending on subphase conditions) which is consistent with an orientation in which the plane of the calixarene ring is parallel to the plane of the water surface. Material **B** shows the strongest interaction with Cu^{2+} and Li^{+} ions when both area per molecule data and effective dipole moment data are considered. The effective dipole moment measured for **B** is significantly larger than that of **A** owing to its highly conjugated fluorenemethylamino system. Furthermore, simple nonconjugated calix[4]arenes investigated by others possessed lower effective dipole moments than those of materials **A** and **B**.

LB deposition is successful for **A** and **B**, but some of the molecular ordering is lost as a result of the transfer onto solid substrates, since the measured surface potentials reduce (typically by 30−50%) for the LB film compared to the floating Langmuir layer. Furthermore, 5 layer LB films exhibit a lower surface potential than the monolayer LB films, suggesting that multilayered films become increasingly disordered. Future work will examine the interaction of these and other similar calix[4]arenes with a range of mono-, di-, and trivalent cations in order to assess the binding capability of LB films of these materials which may find application in ion-contamination measurements within aqueous environments.

Acknowledgment. F.L.S. wishes to acknowledge the Universiti Pendidikan Sultan Idris (UPSI) and Government of Malaysia for the award of a scholarship which enabled her to undertake this work. J.P.W. wishes to thank the Postgraduate R&D Skills Programme and ITT-Dublin's PhD Continuation Fund for grant support.

(25) Korchowiec, B.; Salem, A. B.; Corvis, Y.; Vains, J. B. R. d.; Korchowiec, J.; Rogalska, E. *J. Phys. Chem. B* **2007**, *11*, 13231.
(26) Constantino, C. J. L.; Dhanabalan, A.; O., N. O., Jr. *Colloids Surf., A* **2002**, *198- 200*, 101.
(27) Broniatowski, M.; Latka, P. D. *Colloid Interface Sci.* **2006**, *299*, 916.
(28) Verboom, W.; Durie, A.; Egbenink, R. J. M.; Asfari, Z.; Reinhoudt, D. N. *J. Org. Chem.* **1992**, *57*, 1313.
(29) Creaven, B. S.; Gernon, T. L.; McGinley, J.; Moore, A. M.; Toftlund, H. *Tetrahedron* **2006**, *62*, 9066.